INSTITUTE OF PHYSICS PUBLISHING SUPERCONDUCTOR SCIENCE AND TECHNOLOGY

Supercond. Sci. Technol. **15** (2002) 660–664 PII: S0953-2048(02)33958-7

Interface structure of $YBa_2Cu_3O_x$ thin films prepared by a non-fluorine sol–gel route on a single-domain substrate

Donglu Shi[1], **Yongli Xu**[1], **J Lian**[2], **Lumin Wang**[2] **and Shaun McClellan**[1]

[1] Department of Materials Science and Engineering, University of Cincinnati, Cincinnati, OH 45221-0012, USA
[2] Department of Nuclear Engineering and Radiological Science, University of Michigan, Ann Arbor, MI 48109, USA

Received 16 July 2001
Published 17 April 2002
Online at stacks.iop.org/SUST/15/660

Abstract
In our previous work, we have shown that a single-domain $YBa_2Cu_3O_x$ (YBCO) exhibits a low surface resistance. However, the second phase Y_2BaCuO_5 (211) precipitates inevitably as a result of peritectic reaction. These 211 particles are potential sources of RF losses, which need to be eliminated. In this study, a non-fluorine sol–gel synthesis was developed to deposit a YBCO thin film on the surface of single-domain YBCO. The deposited YBCO thin film entirely covered the 211 particles. The interface structure was studied by high-resolution transmission electron microscopy. The experimental results on sol–gel synthesis and thin film characterization are reported. Also discussed is the underlying mechanism of film growth on single-domain YBCO.

1. Introduction

Low surface resistance, R_s, is a key property of conductors used in RF device applications. For a normal conductor such as copper, the surface resistance is of the order of 0.01 Ω at the frequency of 2 GHz [1–3]. The surface resistance is many orders of magnitude below this at the same frequency range in a well-textured YBCO, making the HTS material an attractive candidate for RF components. To achieve low surface resistance, current approaches in processing HTS are thin film technologies, which can produce epitaxially grown films with a low surface resistance [4–9]. In our previous work we have grown high-quality, single-domain YBCO that exhibits a low surface resistance comparable to those of thin films. With today's technology, such a single-domain YBCO can be readily processed into a dimension up to 60 mm in diameter, which can allow a three-dimensional architecture of the RF component in the device engineering. The advantages also include easy manipulation of the geometry, large cross-sectional area and greater freedom in dimensionality control. These advantages provide unique opportunities in RF component engineering and device design.

Although there have been limited data on the surface resistance of single-domain YBCO, our preliminary experiments have shown quite promising results in this material. As has been reported, the surface resistance of the single-domain YBCO measured at 77 K and 0.8 GHz has reached 0.05 mΩ indicating an extremely low value comparable to those of thin films [10–12]. Such a low surface resistance satisfies the basic requirement in the development of the receiver component. In addition, our previous work has also shown respectable Q values up to 10^4, measured from a substrate-less cavity resonator measured at 18 GHz [11].

There are several challenging issues, however, which need to be addressed in this research. We believe that major energy loss may arise from the dissipation from the second phases such as Y_2BaCuO_5 (211) that is present during the peritectic reaction. Since the 211 particles are non-superconducting, microwave dissipation could become severe in those regions. Therefore, in this research, we have developed a new method to 'cover' the 211 particles by depositing a YBCO thin film on the polished single domain surface. In this method, the single domain YBCO serves as the best compatible substrate and the YBCO film grown on it will have no 211 present in its matrix. In this paper, we report the sol–gel synthesis chemistry and

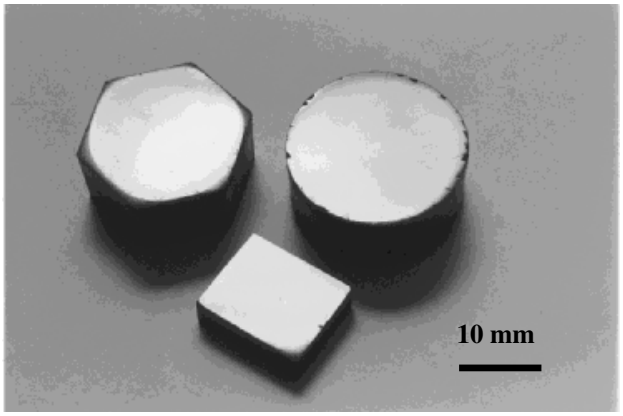

Figure 1. Single domain YBCO prepared by the seeded melt growth method.

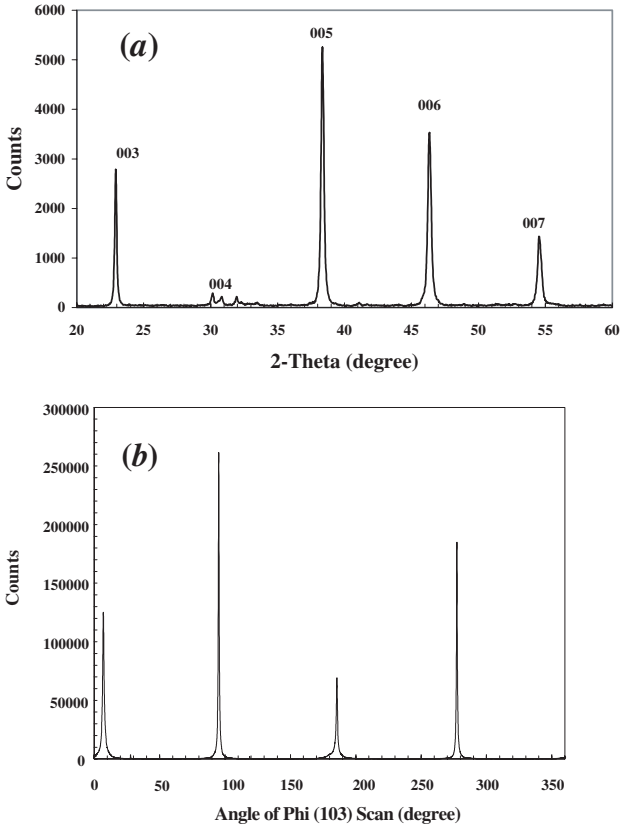

Figure 2. The XRD spectrum of single domain YBCO (*a*) 2 theta scan and (*b*) phi-scan of the (103) peak showing excellent crystallinity of the single-domain YBCO.

characterization of the YBCO thin films by x-ray diffraction (XRD) and high-resolution transmission electron microscopy (HRTEM).

2. Experimental details

Our non-fluorine-based sol–gel YBCO solutions were developed in-house. For the precursor solution, stoichiometric (1:2:3) yttrium trimethylacetate, barium hydroxide and copper trimethylacetate powders were dissolved in a mixed propionic acid/amine solvent with an oxide concentration between 0.1 and 0.5 mol l^{-1}. The addition of amine was important because

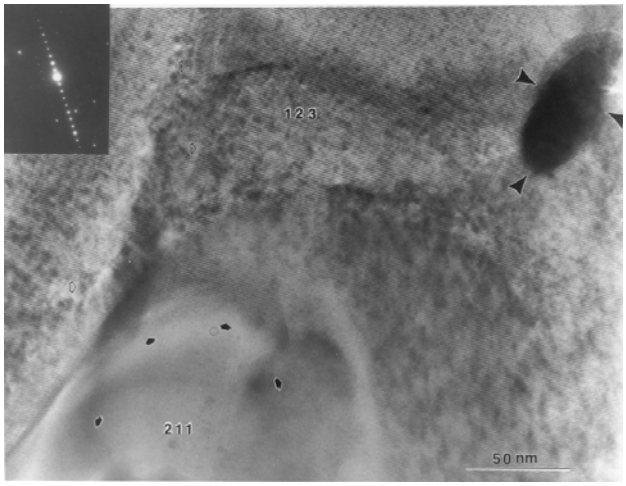

Figure 3. TEM photograph showing the morphology of 211 particles in the matrix of single domain YBCO.

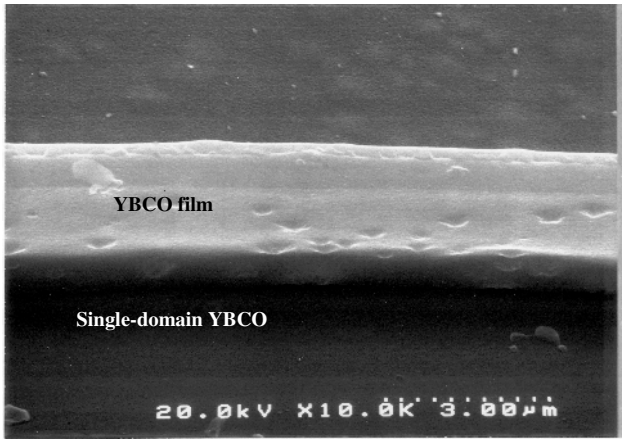

Figure 4. SEM photograph showing the cross section between the YBCO film and the single domain substrate.

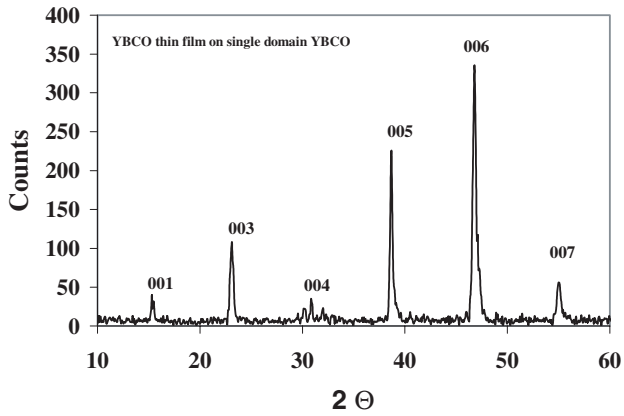

Figure 5. XRD spectrum of the YBCO film on the single domain substrate.

it greatly improved the solubility of the precursor powders in propionic acid. The stock solution was stable in air with a shelf life longer than 2 years. Xylenes of alcohols were used for dilution and for controlling solution viscosity at 10–100 cP. The films on single-domain YBCO were deposited by spin

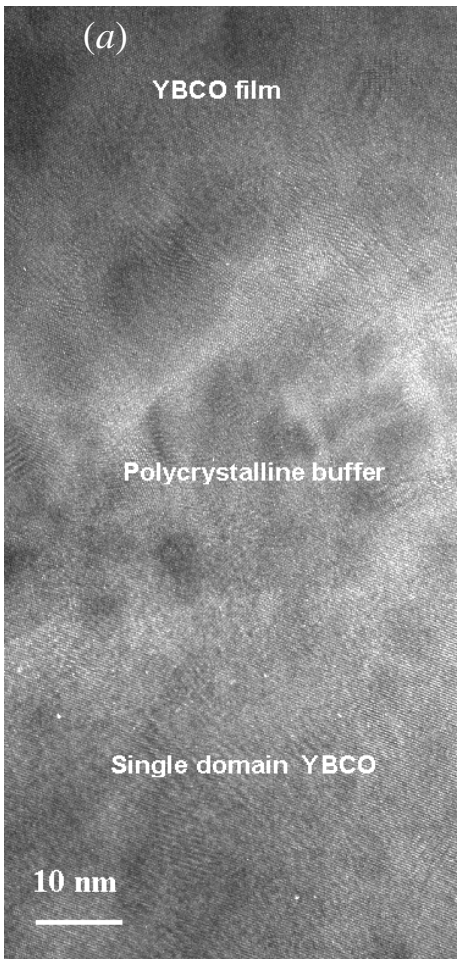

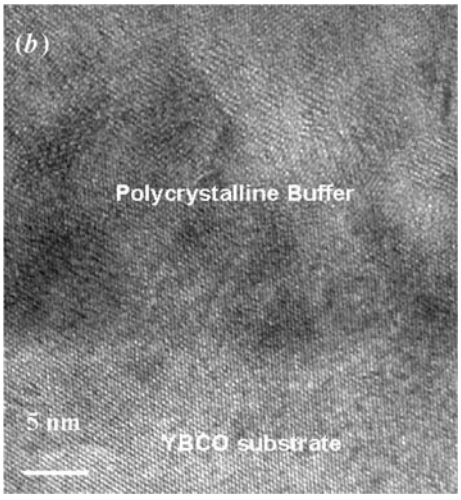

Figure 6. HRTEM photographs showing (*a*) the interface structure between the YBCO film and the single domain substrate. (*b*) A close-up between the buffer layer and the substrate. (*c*) Above the buffer layer the YBCO film appears to grow into a large crystal.

coating at 3000–3500 rpm and were dried at 200–250 °C for several minutes. This process was repeated to build up the desired film thickness (0.5–0.6 μm). The films were heated at 800–920 °C under a controlled atmosphere and O_2 was annealed at 400 °C for 24 h. The single-domain YBCO was grown by the so-called seeded melt growth (SMG) method

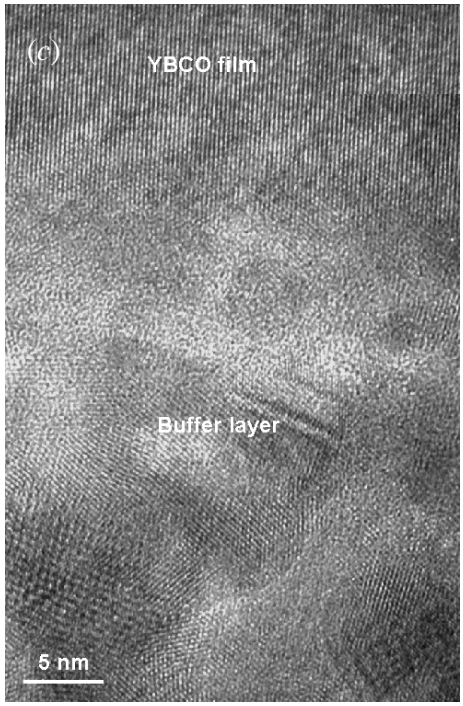

Figure 6. (Continued).

[10–14]. The YBCO substrates were sectioned from a large single-domain material ceramic that was 20 mm in diameter. The substrates were typically 15 × 15 × 3 mm^3 in dimension, and their top surfaces were mirror-polished down to 0.25 μm with diamond paste.

A Philip x-ray diffractometer with Cu Kα radiation was used to carry out the texture investigations. The x-ray wavelength was 1.54 Å with a beam size of 3 mm. Scanning electron microscopy (SEM) experiments were performed on a Hitachi 2000. No conductive coating was applied. The HRTEM experiments were performed on a JEOL JEM 4000EX TEM. Transport resistivity measurements were carried out down to liquid-helium temperature using a standard four-probe method.

3. Results and discussion

Figure 1 shows some typical single domain YBCO substrates processed by the SMG (13, 14). Figure 2 is the 2 theta- and phi-scan of the substrate. These results show the single crystal like characteristics of the domain structure with only (001) peaks in the 2 theta scan (figure 2(*a*)). Figure 2(*b*) is the phi-scan of the (103) peak that indicates the excellent crystallinity of the single domain YBCO. As evident in figure 2(*b*), sharp phi-scan peaks have only 0.63° of the full width at half maxim (FWHM). The TEM (figure 3) photograph reveals the 211 particles in the substrate. These 211 particles range from sub microns to over 10 microns.

Figure 4 shows the cross section of a spin-coated YBCO thin film on the single domain substrate after heat treatment near 900 °C. As can be seen in the SEM photograph, the deposited film has a smooth surface. No sign of negative reactions of large amount of liquids were observed at the interface in the SEM experiments. Figure 5 is the XRD

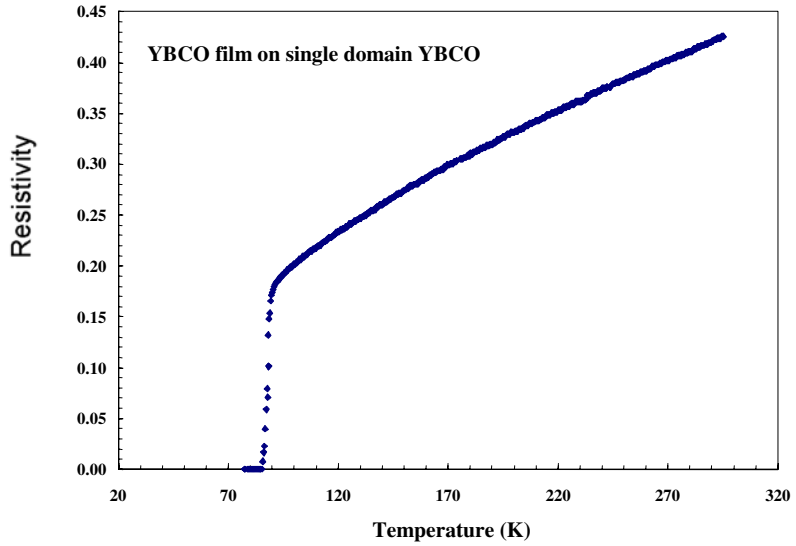

Figure 7. Resistivity versus temperature for the YBCO thin film on single domain YBCO substrate. The units of resistivity are arbitrary. (This figure is in colour only in the electronic version)

spectrum of the YBCO film on the single domain substrate. Almost identical to the XRD spectrum of the substrate shown in figure 2, only (001) peaks are present indicating a well-textured YBCO thin film. It should be noted that the XRD spectrum of an epitaxial YBCO film may well overlap with that of the YBCO substrate as the Cu Kα radiation is quite penetrating. However, comparing figures 2 and 5, we can see that the intensities of the peaks in figure 5 are much weaker than those in figure 2, indicating that the XRD spectrum from figure 5 is likely due to the YBCO film rather than from the YBCO substrate. Figure 6(*a*) is an HRTEM image of the interface between the YBCO film and the YBCO single-domain substrate. The interface exhibits a buffer layer that has been identified as the YBCO structure. The buffer layer extends about 50 nm wide between the film and the substrate, and is polycrystalline in nature. A close-up between the buffer layer and the substrate can be seen in figure 6(*b*). Although the buffer layer has the randomly oriented YBCO nano-crystals, no second phases have been found in this interface area. However, as can be seen in figure 6(*c*), above the buffer layer the YBCO film appears to grow into a large crystal that exhibits a *c*-axis texture characterized by XRD (figure 5).

As shown in figure 3, fine Y_2BaCuO_5 (211) particles disperse in the YBCO matrix with the dimension between sub-micrometres to several hundred micrometres. The 211 particles would certainly pose a different crystal structure, leading to a high degree of lattice mismatch. Depending upon the percentage and dimensions of the 211 particles, the epitaxial growth would suffer from the severe lattice mismatch in many localized areas directly above the 211 phase. Although in figure 6, the image shows the buffer on the YBCO phase, much of the initial nucleation of YBCO could likely take place on the 211 particles. As there is a high density of the 211 particles in the single-domain YBCO matrix, they can act as nucleation sites for the initial crystallization of YBCO. These randomly oriented 211 particles can be responsible for the polycrystalline YBCO buffer layer. However, these nanosize polycrystalline YBCO nuclei would assume extremely high surface energies that need to be minimized by growing into much larger grains. As the buffer layer grows up to a certain thickness, therefore, large crystals form as shown in the top portion of figure 6. Interestingly, these large crystals assume a *c*-axis orientation that is characterized by the XRD spectrum shown in figure 5. It should be noted that the TEM analysis can only focus on small regions at the interface. Although figure 6 represents a typical interfacial structure, it does not preclude other possible epitaxial growth mechanism of YBCO film on the single domain substrate.

As discussed, the source of loss can occur from the 211 regions. To eliminate these non-superconducting regions, we have deposited a thin film of YBCO on the single domain substrate. Since the film was synthesized well below the peritectic temperature, no 211 particles were observed in the matrix of the thin film. This proves to be an effective method in modifying the surfaces of the single domain YBCO for improved RF properties. It should be noted that the peritectic temperature of YBCO is 1010 °C. No severe melting should be expected during the heat treatment of the film between 800 °C and 900 °C. However, it has been reported that there is a eutectic reaction between $BaCuO_2$ and CuO near 870 °C. For a well-grown YBCO single domain, all precursor phases are expected to fully react to form $YBa_2Cu_3O_x$ (123). This should be ensured as the domain growth can take up to 50 h at near peritectic temperature. However, a small amount of liquids may be trapped between the *ab* planes and re-melt upon heating during the film synthesis. Nonetheless, for a *c*-axis single domain, the film is only deposited on the top polished surface and the effects of the liquids are not significant.

The oxygenated film was characterized by the four-probe measurement. The result is shown in figure 7. As can be seen, the film exhibits a typical superconducting transition at near 90 K. However, one may argue that the resistivity data from figure 7 may be affected by the YBCO substrate. Although it is difficult to determine the effects of the substrate from the four-probe measurement, the R versus T curve in figure 7 indicates an overall superconducting YBCO with a T_c near 90 K.

Note here that the film was only oxygenated at 400 °C for 24 h, an annealing time much shorter than the required time for single domain YBCO. Therefore, we believe that it is the YBCO thin film that is responsible for the 90 K transition shown in figure 7. Surface resistance measurement of the YBCO thin film on the single domain substrate is under way.

4. Conclusion

Using a non-fluorine approach we have deposited sol–gel YBCO thin films on a single-domain YBCO by spin coating. The film exhibits a *c*-axis grain texturing confirmed by XRD. The TEM study shows a non-epitaxial growth at the interface and reveals a polycrystalline buffer layer that has been identified as the YBCO structure. The YBCO thin film has a clean interface without any adverse reaction and 211 precipitates. Transport electrical resistivity measurement on the YBCO thin film has shown a superconducting transition near 90 K.

Acknowledgment

This work is supported by an NSF grant under contract No 9802281.

References

[1] Kennedy W K, Zahopoulos C and Sridhar S 1989 *Solid State Commun*. **70** 741
[2] Dubourdieu C, Senateur J P, Thomas O, Weiss F and Müller G 1998 *Physica* C **308** 16–20
[3] Zahopulos C, Kennedy W L and Sridhar S 1988 *Appl. Phys. Lett*. **52** 2168
[4] Phillips J C 1989 *Physics of High-T_c Superconductors* (Boston: Academic)
[5] Missert N *et al* 1989 *IEEE Trans. Magn*. **25** 2418
[6] Li H C, Linger G, Ratzel F, Smithey R and Greerk J 1988 *Appl. Phys. Lett*. **52** 1098
[7] Sandstrom R L, Gallagher W J, Dinger T R and Koch R H 1988 *Appl. Phys. Lett*. **53** 444
[8] Eom C B, Sun J Z, Yamamoto K, Marshall A F, Luther K E, Laderman S S and Geballe T H 1989 *Appl. Phys. Lett*. **55** 595
[9] Lauder A, Myers K E and Face D W 1998 *Adv. Mater.* **10** 1249
[10] Qu D, Shi D, Lu S, Ferendeci A M and Mast D 1999 *Physica* C **315** 36
[11] Shi D, Xu Y, McClellan S and Buchanan R 2001 *Physica* C **354** 71
[12] Qu D, Shi D, Ferendeci A, Mast D, Blackstead H A and Maartense I 2000 *Supercond. Sci. Technol*. **13** 902
[13] Shi D, Zhong W, Welp U, Sengupta S, Todt V, Crabtree G W, Dorris S and Balachandran U 1994 *IEEE Trans. Magn*. **5** 1627
[14] Balachandran U, Zhong W, Youngdahl C A and Peoppel R B 1993 *J. Electron. Mater.* **22** 1285